Electronic Supplementary Information (ESI) for

^{31}P nuclear spin singlet lifetimes in a system with switchable magnetic inequivalence: experiment and simulation

David E. Korenchan[a], Jiaqi Lu[a], Malcolm H. Levitt[b], and Alexej Jerschow*[a]

[a] Department of Chemistry, New York University, New York, NY, USA.
[b] School of Chemistry, University of Southampton, Southampton, UK

Contents

$^{1}H/^{31}P$ NMR spectroscopy of tetrabenzyl pyrophosphate with decoupling

^{31}P and ^{1}H NMR spectra were acquired with decoupling applied on the opposite nucleus during the acquisition time. The ^{1}H NMR spectrum was fitted using the *Spinach* MATLAB package in order to determine the magnitudes of the ^{1}H-^{1}H coupling constant and chemical shift difference. Each methylene ^{1}H pair was modeled as two chemically inequivalent ^{1}H nuclei. Supplementary Figure S1 below shows the results.

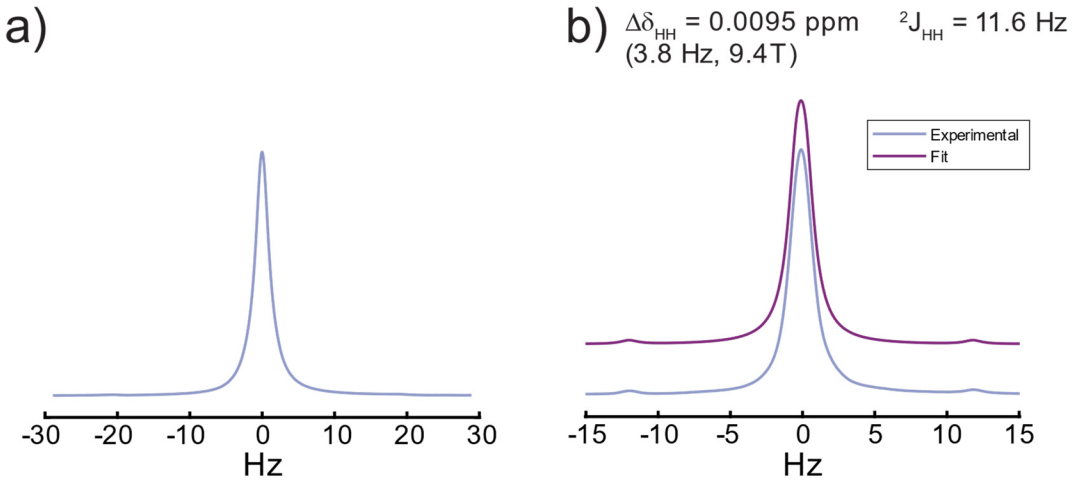

Supplementary Figure S1 – NMR spectra and fitting results with decoupling. (a) ^{31}P NMR spectrum with ^{1}H decoupling applied to the methylene ^{1}H resonance. (b) ^{1}H NMR spectrum with ^{31}P decoupling applied to the ^{31}P multiplet, along with fitted spectrum and corresponding spectral parameters.

SLIC pulse sequence optimization at various temperatures

The SLIC pulse sequence optimization described in the main text was performed at the temperatures used for other experiments in order to see if the optimal SLIC pulse parameters were temperature dependent. Supplementary Figure S2 below demonstrates that there was little variability in either optimal spin-lock pulse power or duration as a function of temperature.

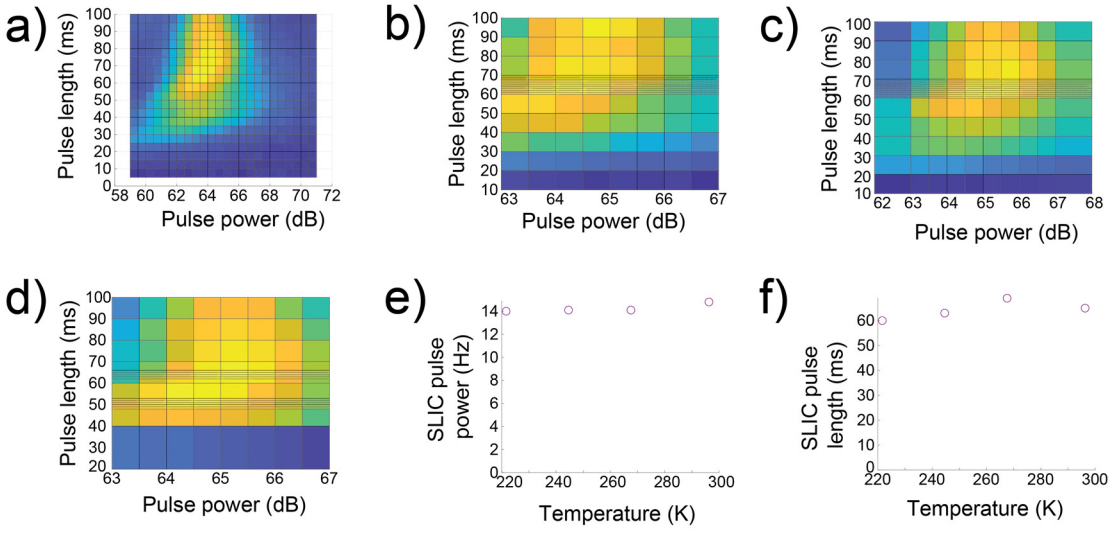

Supplementary Figure S2 – Optimal spin-lock pulse parameters as a function of temperature for singlet-triplet transfer using the SLIC pulse sequence. (a-d) Integrated ^{31}P NMR signal arising from the singlet state as a function of spin-lock pulse power and duration at various temperatures: (a) 296.29 K; (b) 267.56 K; (c) 244.59 K; and (d) 221.61 K. (e) Plot of optimal spin-lock power

as a function of temperature. (f) Plot of optimal spin-lock duration as a function of temperature. All experiments were n = 1 repetition. Note that yellow indicates highest signal intensity. Color bar limits are not matched between separate plots.

SLIC pulse sequence optimization with ^{1}H decoupling applied during spin-lock pulses

In order to test the hypothesis that the ^{31}P singlet state is accessed via the ^{31}P-^{1}H scalar couplings, we measured the signal arising from ^{31}P singlet order as a function of the spin-lock pulse power and duration while applying ^{1}H decoupling at varying powers. The ^{1}H decoupling frequency was set to the methylene ^{1}H resonance. The changes in optimal pulse sequence parameters and overall signal-to-noise ratio are displayed in Supplementary Figure S3 below.

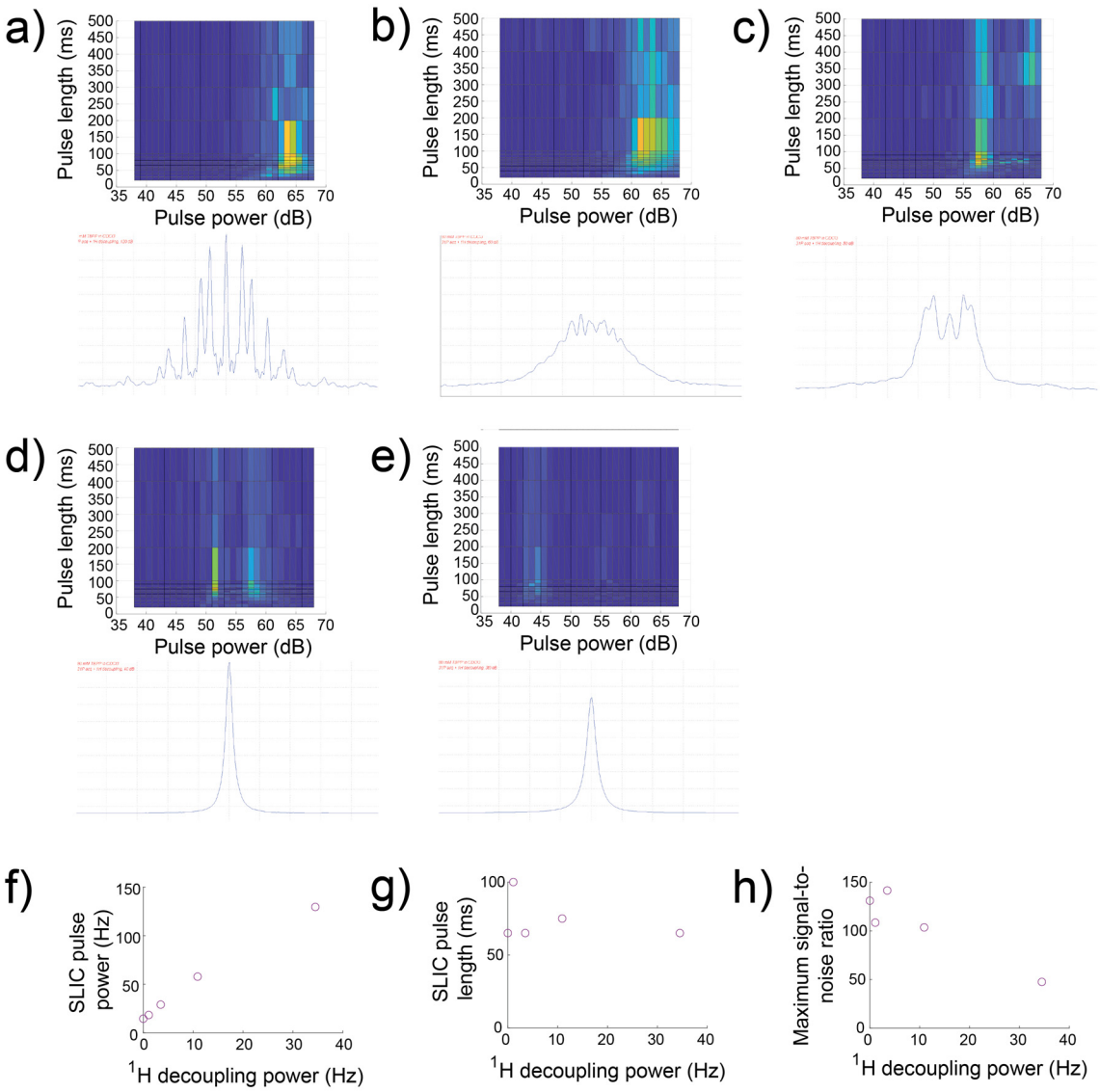

Supplementary Figure S3 – Optimal spin-lock pulse parameters as a function of ^{1}H decoupling power, applied during the spin-lock pulses, for singlet-triplet transfer using the SLIC pulse sequence. (a-e) Integrated ^{31}P NMR signal arising from the singlet state as a function of spin-lock pulse power and duration at ^{1}H decoupling powers: (a) 0 Hz (no decoupling); (b) 1.1 Hz; (c) 3.5 Hz; (d) 10.9 Hz; and (e) 34.5 Hz. The ^{1}H-decoupled ^{31}P NMR spectrum at each decoupling power is displayed below each plot. All plots use the same color scaling for the signal intensities. (f-h) Plots of (f) optimal spin-lock pulse power; (g) optimal spin-lock pulse duration; and (h) maximum signal-to-noise ratio, as a function of ^{1}H decoupling power. All experiments were n = 1 repetition. Note that yellow indicates highest signal intensity. Color bar limits are the same between separate plots.

Table of experimental and simulated R_1 and R_s contributions

The table below summarizes the values shown in Figures 3b-c, both experimental measurements of R_1 and R_s as well as simulated contributions arising from the symmetric and antisymmetric components of the CSA tensor.

Supplementary Table S1 – Experimental values for R_1 and R_s. All measurements were n = 3 except R_1 at 296.29 K (n = 7) and R_1 at 267.56 K (n = 4).

Temperature (K)	Experimental		Experimental	
	R_1, mean (s^{-1})	R_1, standard deviation (s^{-1})	R_s, mean (s^{-1})	R_s, standard deviation (s^{-1})
221.61	1.534	0.185	3.047	0.578
244.59	0.866	0.138	1.820	0.298
267.56	0.547	0.039	1.374	0.287
296.29	0.315	0.006	0.745	0.071

Supplementary Table S2 – Simulated values for R_1 and R_s, including symmetric (^{sim}) and antisymmetric (^{anti}) CSA contributions. Note that the simulated $R^{total} = R^{sym} + R^{anti}$.

Temperature (K)	Simulated			Simulated		
	R_1^{sym} (s^{-1})	R_1^{anti} (s^{-1})	R_1^{total} (s^{-1})	R_s^{sym} (s^{-1})	R_s^{anti} (s^{-1})	R_s^{total} (s^{-1})
220	1.434	0.030	1.464	3.487	0.082	3.5689
240	0.769	0.023	0.792	2.674	0.072	2.7468
260	0.531	0.017	0.547	2.332	0.066	2.3984
280	0.412	0.014	0.425	1.489	0.047	1.5355
300	0.322	0.011	0.333	1.470	0.047	1.5163

CSA tensors for the different conformations

100 conformations were randomly extracted from the MD trajectory. These were equilibrated with Gaussian to find a local minimum in order to avoid overestimates of CSA tensors due to instantaneous vibrations or torsions. Of the 100 conformations 69 converged, and CSA tensors were calculated for these. Supplementary Figure S4 below shows the norms of the symmetric and the antisymmetric components for these conformations for comparison.

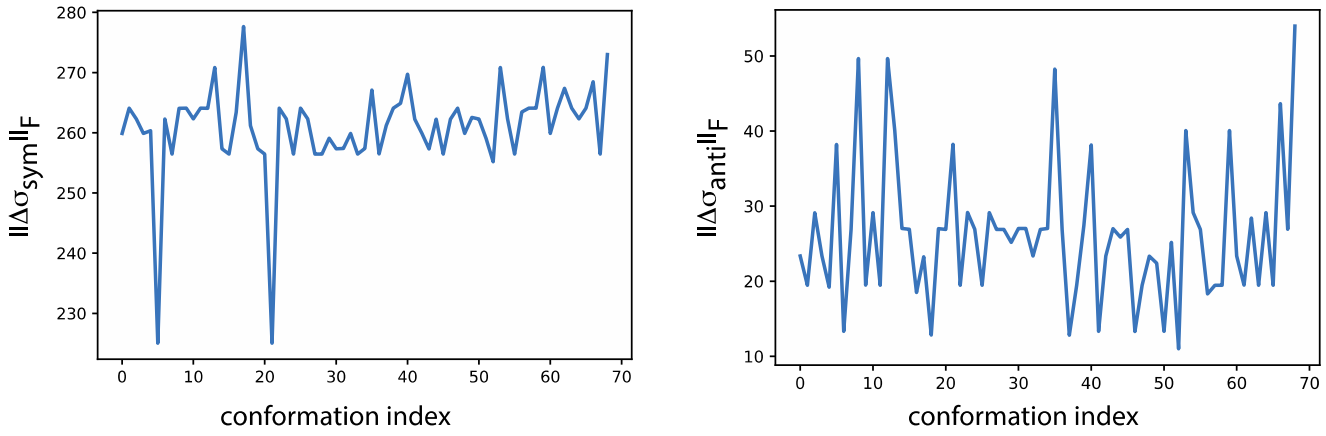

Supplementary Figure S4 – CSA tensor norms of the symmetric and antisymmetric components as a for the 69 conformations considered.

Fitting of experimental and simulated R_1 and R_s as functions of temperature

R_1 and R_s values obtained via experiment or molecular dynamics simulation were fitted as a function of temperature. Motivation of exponential fits of temperature-dependent curves can be provided by the following reasoning: According to Bloembergen-Purcell-Pound (BPP) relaxation theory[1] spin-lattice relaxation is directly proportional to the correlation time, τ_c, in the fast motion regime. Each tetrabenzyl pyrophosphate molecule could be approximated to behave in solution as a spherical particle with hydrodynamic radius r, yielding the following relation:

$$\tau_c = \frac{4\pi\eta(T)r^3}{3kT}$$

In the equation above, T represents temperature, $\eta(T)$ represents viscosity as a function of temperature, and k is Boltzmann's constant. The viscosity can be modeled as a function of temperature according to the Vogel-Fulcher-Tammann equation[2]:

$$\eta(T) = e^{A+\frac{B}{C+T}}$$

The relaxation rate, then, is directly proportional to the exponential factor above and inversely proportional to temperature. The data were fitted accordingly in MATLAB by adjusting the parameters A, B, and C from the equation above. The obtained parameter values are reported in Supplementary Table S3 below. Note that the parameters B and C have been reported previously as 966.0 and 19.02, respectively[3].

Supplementary Table S3 – Fitted parameter values and goodness-of-fit indicators for relaxation rates as a function of temperature, according to Bloembergen-Purcell-Pound theory.

Relaxation Rate	**A**	**B**	**C**	**R^2**
Experimental R_1	1.110	970.9	-15.90	0.9997
Simulated $R_{1,CSA}$	2.238	630.5	-54.38	0.9644
Experimental R_s	2.320	967.6	9.234	0.9918
Simulated $R_{s,CSA}$	3.551	958.8	110.3	0.8570

References

1. N. Bloembergen, E. M. Purcell and R. V. Pound, *Physical Review*, 1948, **73**, 679-712.
2. G. Tammann and W. Hesse, *Z Anorg Allg Chem*, 1926, **156**.
3. DDBST Dortmund Data Bank Software & Separation Technology GmbH, http://ddbonline.ddbst.de/VogelCalculation/VogelCalculationCGI.exe?component=Chloroform